Niu et al. *Zool. Res.* 2024, 45(5): 1037−1047
https://doi.org/10.24272/j.issn.2095-8137.2023.388
https://cstr.cn/32248.14.zr.2024.388

ZR | Zoological Research

Article Open Access

PRSS50-mediated inhibition of MKP3/ERK signaling is crucial for meiotic progression and sperm quality

Chun-Xue Niu[1,#], Jia-Wei Li[1,#], Xiao-Li Li[2], Lin-Lin Zhang[1], Yan Lang[2], Zhen-Bo Song[2,*], Chun-Lei Yu[2], Xiao-Guang Yang[2], Hai-Feng Zhao[3], Jia-Ling Sun[3], Li-Hua Zheng[2], Xue Wang[3], Ying Sun[2], Xiao-Hong Han[3], Guan-Nan Wang[2], Yong-Li Bao[1,*]

[1] *National Engineering Laboratory for Druggable Gene and Protein Screening*, *Northeast Normal University*, *Changchun*, *Jilin* 130117, *China*

[2] *China International Joint Research Center for Human Stem Cell Bank*, *Northeast Normal University*, *Changchun*, *Jilin* 130117, *China*

[3] *Jilin Institute for Drug Control*, *Changchun*, *Jilin* 130022, *China*

ABSTRACT

Serine protease 50 (PRSS50/TSP50) is highly expressed in spermatocytes. Our study investigated its role in testicular development and spermatogenesis. Initially, PRSS50 knockdown was observed to impair DNA synthesis in spermatocytes. To further explore this, we generated PRSS50 knockout (*Prss50*$^{-/-}$) mice (*Mus musculus*), which exhibited abnormal spermatid nuclear compression and reduced male fertility. Furthermore, dysplastic seminiferous tubules and decreased sex hormones were observed in 4-week-old *Prss50*$^{-/-}$ mice, accompanied by meiotic progression defects and increased apoptosis of spermatogenic cells. Mechanistic analysis indicated that PRSS50 deletion resulted in increased phosphorylation of extracellular signal-regulated protein kinases 1 and 2 (ERK1/2) and elevated levels of MAP kinase phosphatase 3 (MKP3), a specific ERK antagonist, potentially accounting for testicular dysplasia in adolescent *Prss50*$^{-/-}$ mice. Taken together, these findings suggest that PRSS50 plays an important role in testicular development and spermatogenesis, with the MKP3/ERK signaling pathway playing a significant role in this process.

Keywords: PRSS50 (TSP50); Meiotic progression; Sperm quality; MKP3; ERK

INTRODUCTION

Infertility affects 8%–12% of couples worldwide, with male factors being a primary or contributing cause in approximately 50% of couples (Agarwal et al., 2015, 2021; Traven et al., 2017). Male fertility relies on the production of morphologically and functionally normal spermatozoa in the testes, their proper maturation in the epididymis, and the efficient functioning of the vas deferens. Testicular failure is a significant cause of infertility (Sharma et al., 2021).

In recent years, the role of serine proteases in spermatogenesis has been extensively studied. Serine protease 55 (PRSS55) and serine protease 37 (PRSS37) are essential for the maturation of sperm surface protein A disintegrin and metalloproteinase 3 (ADAM3) and for sperm migration *in vivo*, with PRSS55 also playing an important role in sperm-egg interaction *in vitro* (Shang et al., 2018; Shen et al., 2013; Zhu et al., 2021). Serine protease 54 (PRSS54) knockout has been shown to reduce male mouse fertility by affecting acrosome deformation and the distribution of acrosomal proteins in the testis and sperm (Shen et al., 2022). Moreover, serine protease 42 (PRSS42/TESSP-2) and serine protease 43 (PRSS43/TESSP-3) are required for meiotic progression and germ cell survival (Yoneda et al., 2013).

Spermatogenesis is a complex process occurring in the testis, requiring the coordinated regulation of testis-specific genes to successfully complete meiosis (Gou et al., 2017; Hou et al., 2016; Sleutels et al., 2012; Takebe et al., 2013; Vasileva et al., 2009). Serine protease 50 (PRSS50) exhibits a testis-enriched expression pattern regulated by methylation in the spermatogenic epithelial cells of humans and mice (Huang et al., 2008). As a cancer-testis antigen, the expression of *Prss50* and its effects on cancer cells have been studied extensively (Cao et al., 2018; Liu et al., 2014; Shan et al., 2002; Song et al., 2011; Xu et al., 2004; Yuan et al., 2015; Zheng et al., 2011). PRSS50 is silenced in spermatogonia, activated in spermatocytes, and silenced in spermatids (Shan et al., 2002; Xu et al., 2004). This fluctuating expression pattern in spermatogenic epithelial cells suggests that PRSS50 likely plays a role in spermatogenesis. Recent studies have demonstrated that PRSS50 is involved in sperm

Received: 23 March 2024; Accepted: 07 April 2024; Online: 08 April 2024

Foundation items: This work was supported by the Research Foundation of Jilin Provincial Science & Technology Development (20210204164YY, YDZJ202201ZYTS524, 20230204067YY, 20230204069YY), Jilin Province Development and Reform Commission (2022C044-3), and Fundamental Research Funds for the Central Universities (135131002)

[#]Authors contributed equally to this work

*Corresponding authors, E-mail: songzb484@nenu.edu.cn; baoyl800@nenu.edu.cn

tail formation (Scovell et al., 2021). However, the role of PRSS50 in testicular tissue development and its underlying molecular mechanisms remain incompletely understood.

In this study, we found that PRSS50 knockout reduced male fertility by impairing testicular development during puberty and disrupting chromatin condensation in the spermatozoa head. Mechanistically, PRSS50 knockdown led to abnormal activation of extracellular signal-regulated protein kinases 1 and 2 (ERK1/2) in spermatocytes, resulting in defects in meiotic progression and the premature formation of haploid spermatids. We also described the phenotype of adolescent *Prss50*$^{-/-}$ mice and clarified the effects of PRSS50 on meiotic progression for the first time. These findings contribute to a comprehensive understanding of the regulatory role of PRSS50 in testicular development and spermatogenesis.

MATERIALS AND METHODS

Ethics approval

All applicable international, national, and/or institutional guidelines for the care and use of animals were strictly followed. All sample collection protocols complied with the current laws of China. All animal procedures performed in this research were reviewed and approved by the Institutional Animal Care and Use Committee of Northeast Normal University (NENU/IACUC), Jilin, China (approval No. 20210922).

Animals and genotyping

The study was approved by the Institutional Animal Care and Use Committee of Northeast Normal University. The generated PRSS50 knockout (*Prss50*$^{-/-}$) (*Tsp50*$^{-/-}$) mice have been reported previously (Li et al., 2024). Adult wild-type and *Prss50*$^{-/-}$ littermates were fed a standard diet and maintained in a temperature- and light-controlled room in accordance. Mice were maintained under specific pathogen-free conditions, with food and water provided *ad libitum*. All mouse tissues were extracted after dislocation of the cervical spine under deep isoflurane anesthesia. DNA was isolated from toe biopsies and used for genotyping with polymerase chain reaction (PCR). The primer sequences for genotyping are listed in Supplementary Table S1.

Cell culture

GC-2spd cells, a mouse-derived spermatogenic line, were kindly provided by the Stem Cell Bank, Chinese Academy of Sciences. HEK 293T and GC-2spd cells were cultured in medium containing 10% fetal bovine serum (Gibco, USA) at 37°C with 5% CO_2.

Establishment of a stable GC-2spd cell line with PRSS50 knockdown

A stable GC-2spd cell line with PRSS50 knockdown was established using lentiviral short hairpin RNA (shRNA) expression. Briefly, shRNA oligonucleotides targeting the PRSS50 open reading frame (ORF) were designed and synthesized using the Lenti-X shRNA Expression System (Clontech, USA), then inserted into the pGreenPuro™ shRNA Cloning and Expression Lentivector containing the puromycin resistance gene using BamHI/EcoRI cloning sites. Subsequently, the lentiviral plasmid expressing shRNA targeting *Prss50*, along with the pMD2.G and psPAX2 plasmids, were co-transfected into HEK 293T cells to produce lentiviral particles using X-tremeGENE HP DNA Transfection Reagent (Roche, Switzerland). The GC-2spd cells were cultured in medium containing recombinant lentiviral particles and polybrene for 48 h, followed by selection with 0.8 μg/mL puromycin.

X-gal staining

An *in situ* β-galactosidase staining kit (RG0039, Beyotime, China) was used for the procedure. Testes were harvested, fixed with ice-cold LacZ fixture buffer, and incubated for 2 h in fixing buffer at 4°C on a shaking platform. After washing twice (10 min each time) with LacZ washing buffer, the testes were incubated with LacZ staining buffer overnight at room temperature. Subsequently, the tissues were fixed, sectioned, and subjected to nuclear staining with Nuclear Red.

Histological analysis

Mouse testes were removed, weighed, fixed in modified Davidson's Fixative (mDF), and processed in paraffin according to standard methods. Paraffin-embedded testis sections (5 μm) (n≥6) were subjected to gradient ethanol dewaxing and stained with hematoxylin and eosin (H&E) for histological examination. For immunohistochemical analysis, a two-step IHC detection kit (PV-6001, China) was used. Paraffin-embedded testis sections (5 μm) (n=3) were deparaffinized and rehydrated using an ethanol gradient, followed by incubation with hydrogen peroxide for 15 min to quench endogenous peroxidase activity. The sections were then washed three times with phosphate-buffered saline (PBS) and incubated with anti-PRM2 antibody (ATL-HPA056386, Altas, Sweden). The sections were again washed with PBS and incubated in reaction enhancer. Finally, 3,3'-diaminobenzidine (DAB) was used as the chromogen and hematoxylin was applied as a counterstain.

Immunofluorescence

Mouse testis tissues (n≥6) were fixed with 4% paraformaldehyde, embedded in optimal cutting temperature (OCT), permeabilized with 0.1% Triton X-100 in PBS, and blocked with bovine serum albumin (BSA). The sections were then incubated with anti-PRSS50 (ab181993, Abcam, USA), anti-SCP3 (ab97672, Abcam, USA), anti-gamaH2A.X (ab22551, Abcam, USA), and anti-SCP3 (23024-1-AP, Proteintech, USA). Subsequently, Cy3-conjugated and FITC-conjugated secondary antibodies were used for staining, with nuclei counterstained with 4',6-diamidino-2-phenylindole (DAPI).

Immunoblotting analysis

The testes (n≥6) were harvested and lysed with cell lysis buffer. Samples (50 μg protein/lane) were subjected to sodium dodecyl sulfate-polyacrylamide gel electrophoresis (SDS-PAGE) and transferred onto polyvinylidene fluoride (PVDF) membranes. The membranes were blocked with 5% non-fat dry milk for 1 h at room temperature and subsequently incubated overnight at 4°C with rabbit anti-PRSS50 (1:1 000; ab181993, Abcam, USA), ERK1/2 (1:1 000; #4695, CST, USA), p-ERK1/2 (1:1 000; #4370, CST, USA), and MAP kinase phosphatase 3 (MKP3) (1:1 000; ab76310, Abcam, USA). The membranes were then incubated with a horseradish peroxidase-conjugated goat anti-mouse IgG (1:2 000; SA00001-1, Proteintech, USA) or goat anti-rabbit (1:2 000; SA00001-2, Proteintech, USA) for 1 h at room temperature. Chemiluminescence was detected using an enhanced chemiluminescence (ECL) blot detection system (Canon, Japan).

Enzyme linked immunosorbent assay (ELISA)

Blood was obtained by cardiocentesis from anesthetized mice (*n*=3), then centrifuged at 4°C, 3 000 ×*g* for 20 min for serum collection. Similarly, mouse testicular tissue (*n*=3) was cut into pieces in PBS and centrifuged for supernatant collection. The levels of follicle stimulating hormone (FSH), estradiol (E2), luteinizing hormone (LH), and testosterone (T) were measured using an ELISA kit (ml001910, ml001962, ml063366, and ml001948, Mlbio, China). All experiments were repeated three times and the average value was taken.

Spermatocyte nuclear spreading

Mouse testes (*n*=6) were harvested, and the tunica albuginea was removed. The seminiferous tubules were treated with hypotonic extraction buffer (30 mmol/L Tris, 50 mmol/L sucrose, 17 mmol/L trisodium citrate dihydrate, 5 mmol/L ethylenediaminetetraacetic acid (EDTA), 0.5 mmol/L dithiothreitol, and 0.5 mmol/L phenylmethylsulfonyl fluoride (PMSF); pH 8.2) for 40 min, then homogenized in 60 μL of 100 mmol/L sucrose buffer (pH 8.2). The fragmented testicular tubules were resuspended in 100 mmol/L sucrose and dispersed into single cells. The cell suspension was added to the bottom corner of a slide, spread along the length and width of the slide to cover it completely, and immediately placed flat in a humidified chamber. The slides were dried and stored at −80°C for immunofluorescence.

Reverse transcription-quantitative real-time polymerase chain reaction (RT-qPCR)

Mouse testes (*n*=6) were harvested, and total RNA was extracted using Trizol reagent (Invitrogen, USA). RNA was reverse-transcribed to cDNA using a cDNA synthesis kit (Transgene, China) and qPCR was performed using SYBR green on machine (PikoReal 96, Thermo Fisher Scientific, USA).

The cycling conditions were started with 95℃ for 10 min, followed by 40 cycles at 95°C for 15 s and 60°C for 1 min. The qPCR values were normalized to a housekeeping gene. Fold-change in gene expression was calculated using the $2^{-\Delta\Delta Ct}$ method (Livak & Schmittgen, 2001). The primer sequences for qPCR are summarized in Supplementary Table S2.

Terminal deoxynucleotidyl transferase mediated dUTP nick end labeling (TUNEL)

Mouse testes (*n*=3) were fixed with mDF, after which 5 μm paraffin-embedded testis sections were deparaffinized and rehydrated. Apoptosis was evaluated using the TUNEL assay with an *In situ* Direct DNA Fragmentation Assay Kit (DeadEnd™ Fluorometric TUNEL System, G3250, Promega, USA). According to the manufacturer's protocol, testis sections were incubated with proteinase K for 10 min at room temperature and washed with PBS. Sections were then incubated with terminal deoxynucleotidyl transferase and rTdT buffer at 37°C for 1 h. Finally, the sections were washed three times (5 min each time) with PBS and counterstained for 10 min at room temperature with DAPI. TUNEL staining was visualized using a confocal microscope. Negative and positive staining controls were included in each experiment. All histological procedures were performed blindly.

Sperm counting

The epididymis tail (*n*=6) was minced in 1 mL of PBS at 37°C for 20 min to release sperm into the medium. The total number of sperm in the final suspension was counted with a hemocytometer.

Co-immunoprecipitation

Lysate samples were immunoprecipitated with rabbit anti-MKP3 (1:40; ab76310, Abcam, USA) and rabbit anti-ERK1/2 (1:40; #4695, CST, USA) at 4°C overnight, followed by incubation with protein A/G agarose (Beyotime, China) beads at 4°C for 2 h. The agarose beads were then collected by centrifugation at 4°C ,1000 rpm, after washing 5 times (5 min each time) with PBST, resuspended in sample buffer. Bound proteins were resolved by SDS-PAGE, followed by western blot analysis as described above. IgG (Beyotime, China) was provided as a negative control.

Statistical analyses

Statistical analyses were performed using GraphPad Prism (v.9). All data were obtained from three independent experiments and presented as mean±standard deviation (SD). *P*-values were calculated using two-tailed, paired student's *t*-test, with $P<0.05$ considered significant.

RESULTS

PRSS50 knockdown affected DNA synthesis capacity of GC-2spd cells

We hypothesize that PRSS50 plays an important role in spermatocytes due to its exclusive expression in these cells compared to other spermatogenic cells (Xu et al., 2004). The immortalized mouse spermatocyte cell line GC-2spd was used in this study. The high expression of PRSS50 was initially confirmed in the GC-2spd cells (Figure 1A), after which stable PRSS50-knockdown GC-2spd cells were generated to investigate the role of PRSS50 (Figure 1B, C). Results indicated that PRSS50 knockdown inhibited DNA synthesis and decreased the viability of GC-2spd cells (Figure 1D, E). In addition, increased cell apoptosis was detected in PRSS50-knockdown GC-2spd cells, suggesting that PRSS50 plays an important role in the viability of spermatocytes.

PRSS50 knockout reduced fertility in male mice

To determine the role of PRSS50 in male reproduction, *Prss50*$^{-/-}$ mice were generated and genotyped using PCR (Figure 2A; Supplementary Figure S1A). The knockout efficiency of PRSS50 was confirmed using immunoblotting and immunofluorescence, demonstrating successful establishment of PRSS50 knockout mice (Figure 2C, D). To evaluate male fertility, 2-month-old wild-type and *Prss50*$^{-/-}$ male mice were mated with wild-type females with proven fertility for one week. Successful conception was identified by the presence of a vaginal plug and subsequent abdominal growth (Chen et al., 2015), with litter sizes recorded upon delivery. Results indicated that while the number of offspring from knockout mice was significantly reduced, there were no instances of complete sterility among *Prss50*$^{-/-}$ mice (Figure 2E). This finding contrasts with previous research reporting 20% sterility in *Prss50*-null male mice (Scovell et al., 2021). Overall, these results suggest that the presence of PRSS50 is essential for maintaining fertility in male mice.

PRSS50 knockout resulted in abnormal sperm structure in male mice

Given the observed impairment in fertility, the structure and sperm count of the epididymis were examined, revealing no significant differences between wild-type and *Prss50*$^{-/-}$ mice (Figure 3A, B). Previous studies have reported a significant reduction in sperm motility in the absence of *Prss50* (Scovell

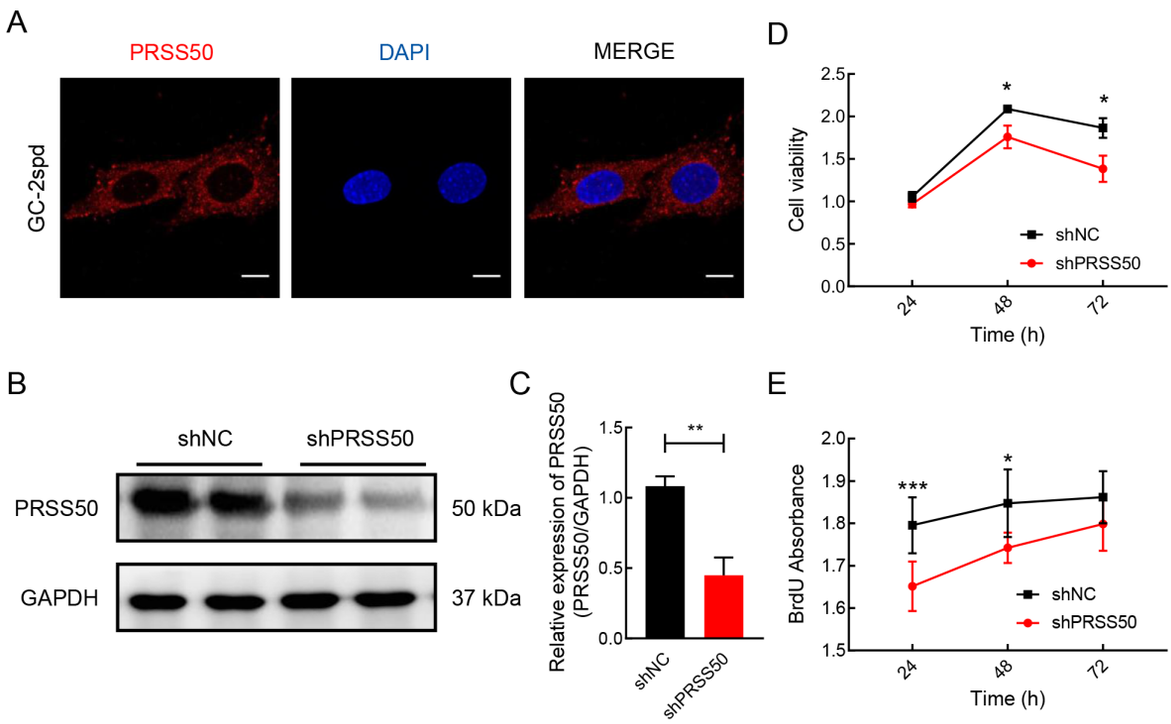

Figure 1 Serine protease 50 (PRSS50) knockdown affected DNA synthesis in GC-2spd cells

A: Immunofluorescence analysis of GC-2spd cells showed PRSS50 localization in the cytoplasm. Scale bar: 20 μm. B, C: Western blot analysis showed that PRSS50 was down-regulated in PRSS50-knockdown GC-2spd cells. D: Methylthiazolyldiphenyl-tetrazolium bromide (MTT) assay showed that cell viability was reduced in PRSS50-knockdown GC-2spd cells. E: 5-Bromo-2-deoxyuridine (BrdU) incorporation assay showed that DNA synthesis capacity was reduced in PRSS50-knockdown GC-2spd cells. Data are mean±SD, *: P<0.05; **: P<0.01; ***: P<0.001.

et al., 2021). Sperm motility is crucial for successful fertilization and is significantly associated with the expression ratio of protamine 1 (*Prm1*) and protamine 2 (*Prm2*), two sperm nuclear proteins crucial for the correct packaging of paternal DNA (Aoki et al., 2006; Hammoud et al., 2009; Moghbelinejad et al., 2015). *Prm1* and *Prm2* gene expression facilitates the compaction and condensation of genetic material within the developing spermatid. When *Prm2* expression is lower than *Prm1* expression, genetic material binds more tightly in the nucleus (Lüke et al., 2014). We tested the *Prm2*/Prm1 ratio in the epididymis and testes of adult mice and found an increased ratio in the testes of 6-week-old *Prss50*$^{-/-}$ mice and in the epididymis of 8-week-old of *Prss50*$^{-/-}$ mice (Figure 3C–F). This finding correlated with the observation of loose spermatid nuclei when analyzing testicular ultrastructure. In the testes of 8-week-old *Prss50*$^{-/-}$ mice, some spermatid nuclei exhibited uneven nuclear chromatin concentration, slightly dented edges, and unclear acrosomal coverage (Figure 3G). Overall, these data indicate that disrupted spermatid nuclear condensation is a contributing factor to reduced fertility in *Prss50*$^{-/-}$ mice.

PRSS50 maintained normal testicular development in adolescent male mice

The ratio of testes weight to body weight was next examined in juvenile mice, revealing that testis size was significantly smaller only in 4-week-old *Prss50*$^{-/-}$ mice (Figure 4A). Consequently, testicular tissue from mice at this age was evaluated. Compared to wild-type mice, *Prss50*$^{-/-}$ mice exhibited smaller testicular tissue volume (Figure 4B) and thinner seminiferous tubules (Figure 4C, D). Given the critical role of reproductive hormones in meiosis and spermatogenesis (Plant & Marshall, 2001; Shiraishi & Matsuyama, 2017; Smith & Walker, 2014), the levels of T, FSH, LH, and E2 were measured in adolescent male mice. Results indicated that the levels of FSH, E2, and LH in serum, as well as the level of T secreted by Sertoli cells in the testis, were significantly lower in *Prss50*$^{-/-}$ mice compared to wild-type mice (Figure 4E–H). As sex hormones are also steroids, the expression levels of steroid synthase genes and hormone receptors were further examined. Results showed that the expression of steroid synthase genes was significantly decreased in *Prss50*$^{-/-}$ mice (Figure 4I), while the mRNA level of hormone receptors did not change significantly (Supplementary Figure S2H). Additionally, when the same indicators were examined in 8-week-old mice, no significant differences were found between *Prss50*$^{-/-}$ and wild-type mice (Supplementary Figure S2A–G). These results suggest that PRSS50 plays a vital role in testicular development and hormone secretion during puberty.

PRSS50 was required for meiotic progression

Proliferation marker protein Ki-67 (Ki67) is exclusively expressed in spermatogonia within the spermatogenic epithelium (Huang et al., 2016). Examination of Ki67 expression in testicular tissue sections found no significant differences between wild-type and *Prss50*$^{-/-}$ mice (Supplementary Figure S3A), consistent with previous research (Scovell et al., 2021). As the absence of PRSS50 had no effect on spermatogonia proliferation, meiotic progression in spermatocytes was next investigated. The mRNA levels of stimulated by retinoic acid gene 8 (*Stra8*), which controls meiosis initiation, were significantly reduced in *Prss50*$^{-/-}$ mice at 2 weeks post-birth, indicating that PRSS50 plays an important role in meiosis initiation (Supplementary Figure S3B). *In vitro* studies demonstrated impaired DNA

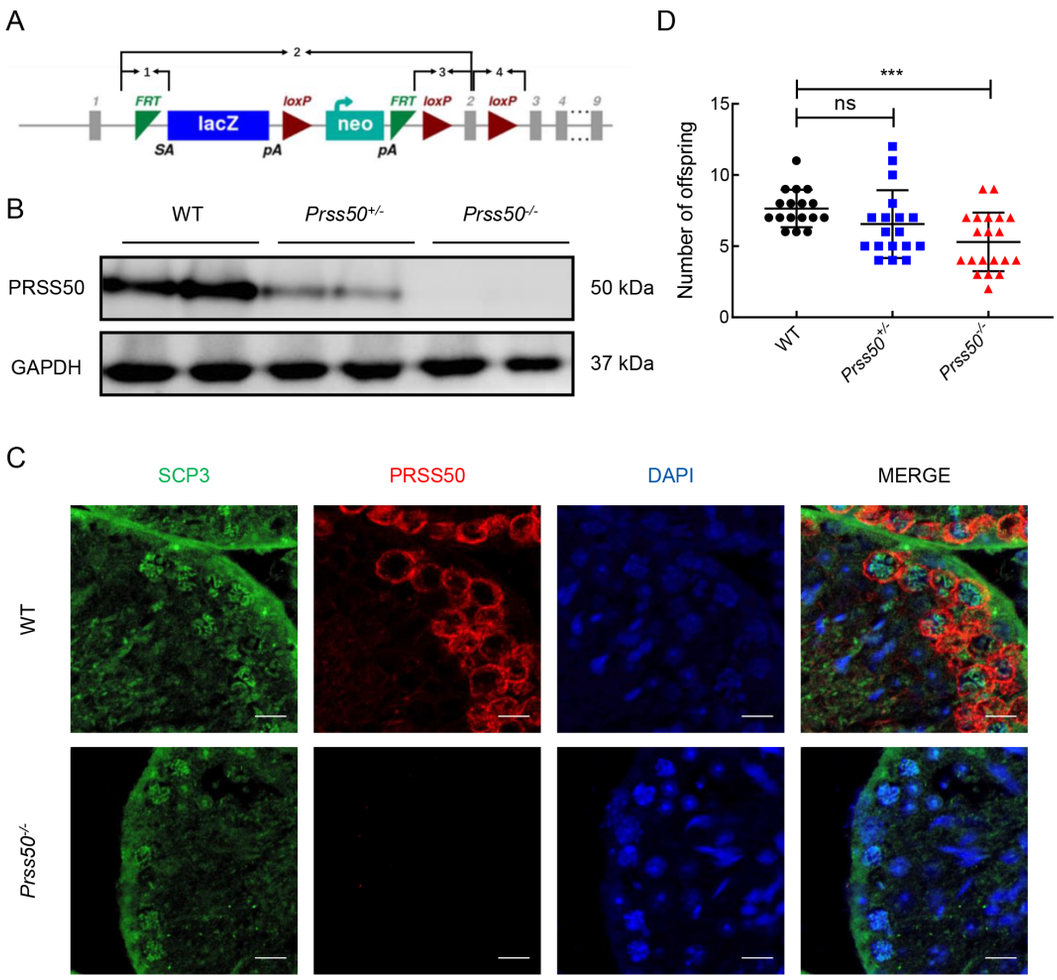

Figure 2 PRSS50 knockout affected fertility in 8-week-old male mice

A: *Prss50*$^{-/-}$ mice were generated by inserting IRES-LacZ and neomycin-resistance gene before the second exon. B: Western blot analysis showed that PRSS50 was not expressed in testis of *Prss50*$^{-/-}$ mice. C: Immunofluorescence analysis showed that PRSS50 was not expressed in spermatocytes. Scale bar: 20 μm. D: Number of offspring of male littermate mice decreased in *Prss50*$^{-/-}$ mice. Data are mean±SD, ns: Not significant; ***: P<0.001.

synthesis in spermatocytes, suggesting potential effects on the meiotic process. Meiosis I is the phase of DNA synthesis, during which γH2AX marks sites of DNA damage across the nucleus, remaining on the sex chromosomes as DNA is repaired. SCP3, a key component of the synaptic complex, is often used as synapsis marker. Nuclear spreading of spermatocytes and immunofluorescence staining for SCP3 and γH2A.X (Figure 5A) demonstrated higher percentages of spermatocytes during the leptotene and zygotene stages in 4-week-old *Prss50*$^{-/-}$ mice compared to wild-type mice, with the opposite observed during the pachytene and diplotene stages (Figure 5B–E). These results suggest meiotic blockage at the zygotene to pachytene stage in some spermatocytes. Increased apoptosis of spermatogenic cells in *Prss50*$^{-/-}$ mice was evidenced by elevated TUNEL-positive cells in seminiferous tubules at postnatal 4 weeks (Figure 5F, G). Furthermore, haploid cell marker expression was abnormally elevated in the testes of *Prss50*$^{-/-}$ mice during puberty, indicating the formation of abnormal spermatids (Figure 5H). Correct spatiotemporal expression of protamine is crucial for spermatid nuclear condensation, with the abnormal expression of PRM2 in *Prss50*$^{-/-}$ mice suggesting premature nuclear remodeling and chromatin condensation (Figure 5I). Collectively, these findings suggest that spermatocytes in *Prss50*$^{-/-}$ mice may bypass critical steps in the meiotic process, leading to impaired spermatogenesis and reduced fertility.

PRSS50 affected meiosis by binding to MKP3

Previous reports have shown that MAPK/ERK1 signaling pathway activation is essential for the meiosis of spermatocytes (Sette et al., 1999). To investigate whether PRSS50 knockdown affects this signaling pathway, we examined p-ERK1/2 protein levels in GC-2 cells. Results indicated a remarkable increase in p-ERK1/2 protein levels in shPRSS50 cells (Figure 6A, B), consistent with observations in 4-week-old mice (Supplementary Figure S4A). To further clarify the mechanism by which PRSS50 regulates the ERK1/2 signal, the interaction between PRSS50 and ERK1/2 was detected by co-immunoprecipitation. Results showed that PRSS50 did not bind to the ERK1/2 protein (Supplementary Figure S4B). Mitogen-activated protein kinase phosphatases (MKPs) are a family of enzymes that dephosphorylate ERK (Camps et al., 2000). As MKP1 and MKP2 are located in the nucleus, while MKP3 is localized in the cytoplasm, MKP3 protein levels were measured in GC-2 cells. Results indicated that the expression of MKP3 was elevated in shPRSS50 cells compared to shNC cells (Figure 6C, D), as observed in 4-week-old mice (Supplementary Figure S4C). In addition,

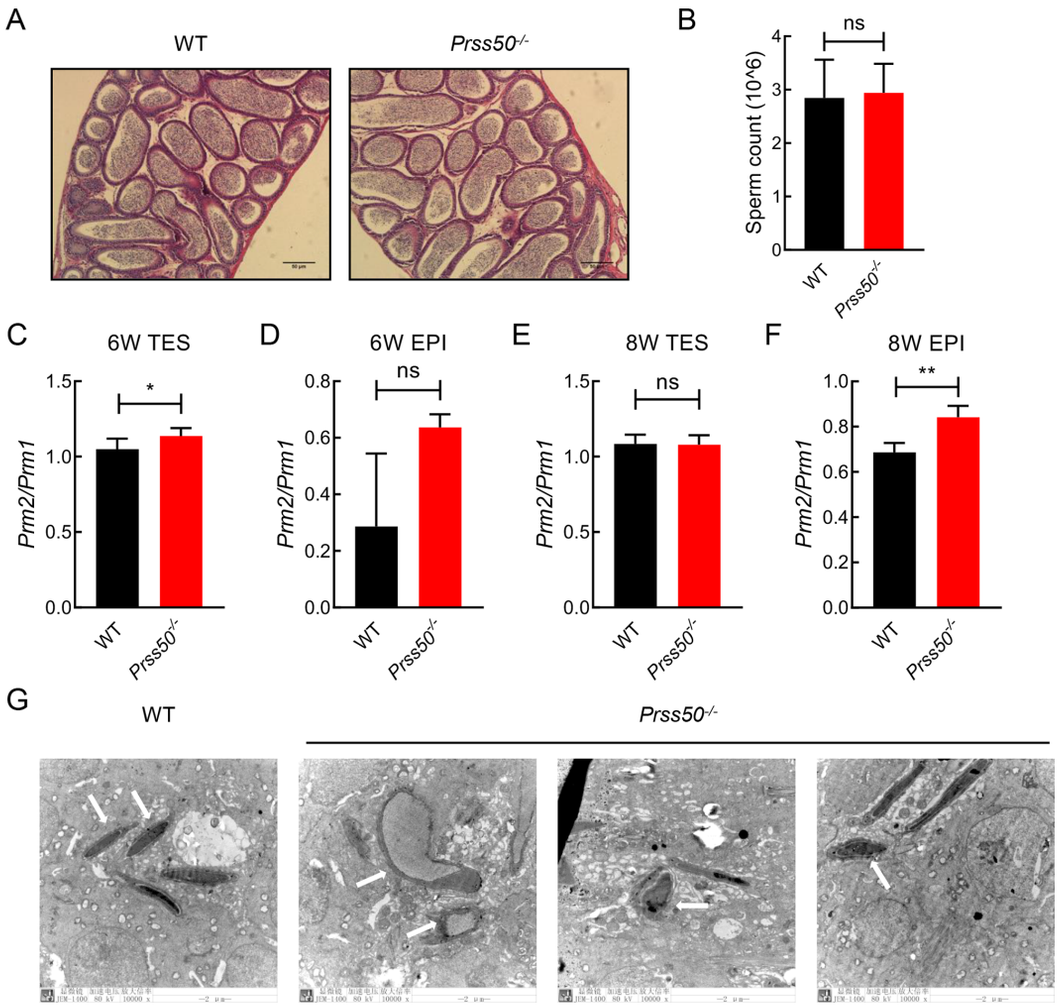

Figure 3 PRSS50 knockout impaired sperm production

A, B: There were no differences in sperm count between wild-type and *Prss50*$^{-/-}$ mice as measured by H&E-staining of the epididymis. Scale bar: 50 μm in A. C: *Prm2*/*Prm1* ratio was increased in the testis of 6-week-old *Prss50*$^{-/-}$ mice. D: *Prm2*/*Prm1* ratio was detected in the epididymis of 6-week-old wild-type and *Prss50*$^{-/-}$ mice. E: *Prm2*/*Prm1* ratio was detected in the testis of 8-week-old wild-type and *Prss50*$^{-/-}$ mice. F: *Prm2*/*Prm1* ratio was increased in the epididymis of 8-week-old *Prss50*$^{-/-}$ mice. G: Ultrastructure of spermatid nuclei (white arrows) was assessed by transmission electron microscopy (TEM). Scale bar: 2 μm. Wild-type mice showed normal spermatid nuclei, *Prss50*$^{-/-}$ mice showed loose spermatid nuclei. Data are mean±SD, ns: Not significant; *: P<0.05; **: P<0.01.

immunofluorescence assays demonstrated that PRSS50 was co-localized with MKP3 (Figure 6E), with co-immunoprecipitation confirming that these two proteins formed a complex (Figure 6F), consistent with observations in 4-week-old mice (Supplementary Figure S4D). To determine whether PRSS50 influences the stability of MKP3, the half-life of MKP3 was measured following inhibition of *de-novo* protein synthesis by cycloheximide (CHX). Results showed that the half-life of MKP3 was significantly extended in shPRSS50 cells (Figure 6G, H). The effect of PRSS50 on MKP3 phosphatase activity was also examined. Both shNC and shPRSS50 cells were treated with BCI, an MKP3 inhibitor, with the level of p-ERK found to be not significantly increased in shPRSS50 cells (Figure 6I, J). In summary, these findings suggest that PRSS50 maintains the phosphatase activity of MKP3 by binding to it. In the absence of PRSS50, the inhibitory effect of MKP3 on ERK1/2 activation is alleviated.

DISCUSSION

In this study, we demonstrated the critical role of serine protease PRSS50 in regulating meiotic progression and haploid cell formation. Notably, deletion of PRSS50 impaired the phosphatase activity of MKP3, leading to elevated phosphorylation levels of ERK1/2. This disruption led to arrested meiosis in spermatocytes and incomplete condensation of the spermatid nucleus, ultimately compromising fertility in male mice.

Basic proteins that bind sperm DNA are essential for mouse reproduction (Cho et al., 2001, 2003). Aberrant localization and premature expression of *Prm2* and *Tnp2* result in abnormal spermatid elongation and failure to complete spermatid differentiation (Malla & Bhandari, 2017). Removal of translational inhibition of *Prm1* causes premature accumulation of PRM1 protein, leading to arrest of spermatid differentiation and dominant male sterility (Lee et al., 1995). Our results showed that premature expression of genes involved in histone-protamine exchange in *Prss50*$^{-/-}$ mice led to impaired spermatid nucleus formation, abnormal spermatocyte meiosis, and reduced offspring of male mice.

Adolescence represents a critical period in the development of the male reproductive system, during which testicular tissue is highly sensitive to sex steroid hormones (Perobelli, 2014).

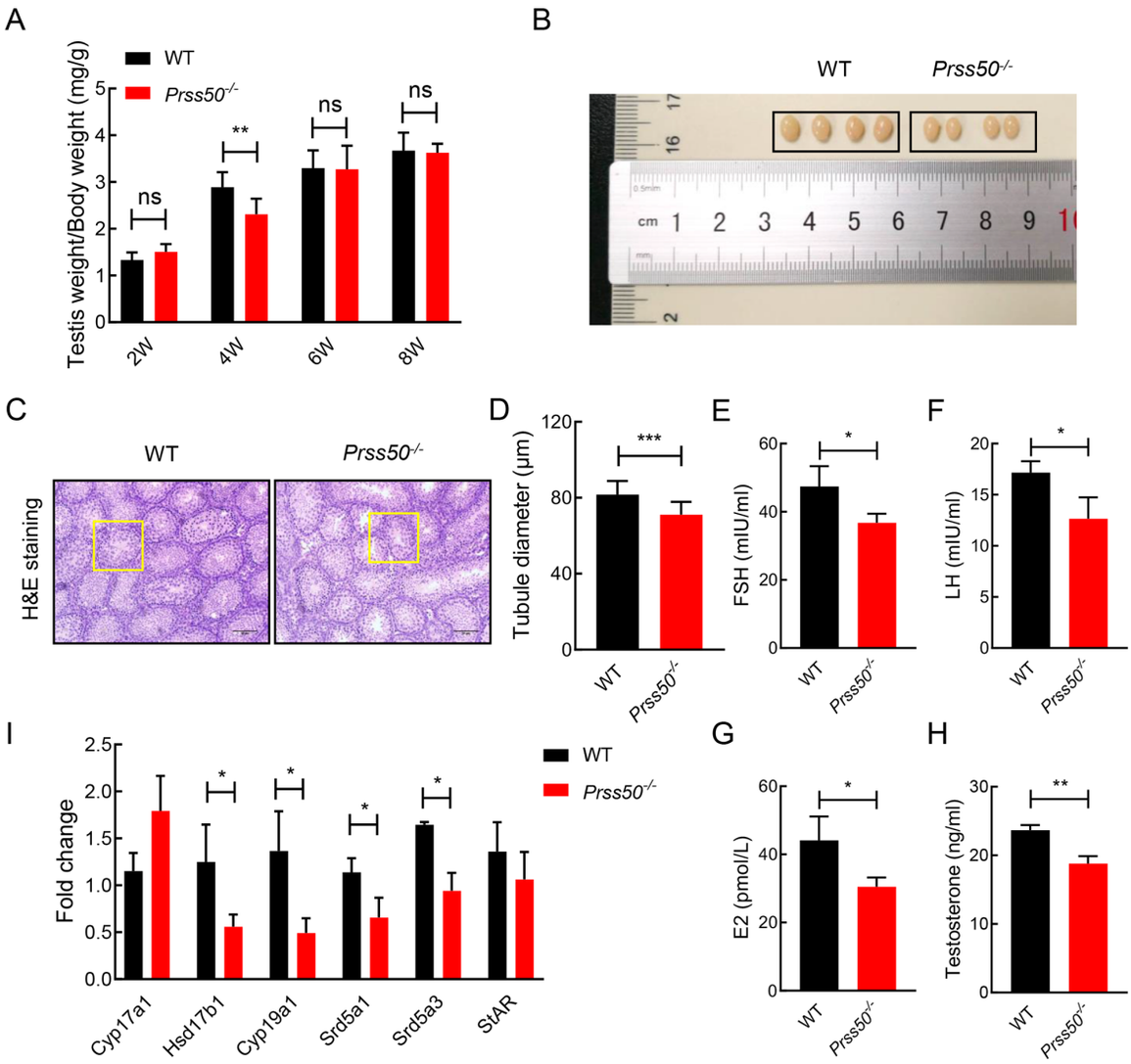

Figure 4 PRSS50 knockout retarded testicular tissue development in 4-week-old mice

A: Statistical analysis showed that the testis weight/body weight ratio of 4-week-old *Prss50*$^{-/-}$ mice was decreased. B: Testes size of 4-week-old *Prss50*$^{-/-}$ mice was smaller than that of wild-type mice. Photo by Chun-Xue Niu. C, D: Wild-type mice showed normal spermatogenic tubule structure, while testes of *Prss50*$^{-/-}$ mice showed thinner spermatogenic tubules. Scale bar: 50 μm in C. E–H: Levels of follicle stimulating hormone (E), luteinizing hormone (F), and estradiol (G) in serum and testosterone level (H) in testicular tissue were reduced in *Prss50*$^{-/-}$ mice based on ELISA. I: mRNA levels of steroid synthase genes were reduced in testicular tissue of *Prss50*$^{-/-}$ testes based on qPCR assay. Data are mean±SD, ns: Not significant; *: P<0.05; **: P<0.01; ***: P<0.001.

Hormones such as T, FSH, and LH are pivotal for testicular growth (Koskenniemi et al., 2017). Maturation of the adult male reproductive system requires proper spatiotemporal expression of sex hormones during puberty (Clark & Cochrum, 2007). Steroidogenesis activating lncRNA in testis (*Start*) is located within the same *Prss/Tessp* locus as *Prss50* in mice, where it activates steroid synthase genes and influences T synthesis. Similar to *Prss50*, *Start* knockout mice exhibit different phenotypes before and after adulthood, a similarity largely attributed to their genetic homology. This suggests that the mechanism by which *Prss50* regulates sex hormones may be analogous to that of *Start* (Otsuka et al., 2021).

The MAPK signaling pathway is important in the reproductive system (Hacioglu et al., 2017; Sommerer et al., 2005), with ERK activation functioning independently of other molecules (Sommerer et al., 2005). The ERK signaling pathway is known to mediate smoking-induced cell cycle arrest and cell death in GC-2spd cells (Esakky et al., 2015), and its activation promotes the proliferation of spermatogenic cells (Dolci et al., 2001; Falvo et al., 2022). In this study, PRSS50 knockdown in GC-2spd cells resulted in reduced DNA synthesis capacity despite increased ERK phosphorylation. This suggests that continuous activation of this pathway may be necessary to maintain cell survival following PRSS50 knockdown. Previous research has shown that ERK activation is involved in meiotic progression and the regulation of germ cell fate (Guida et al., 2022; Sette et al., 1999; Tassinari et al., 2015). The observed increase in ERK phosphorylation may be due to a higher number of spermatocytes undergoing meiosis. PRSS50 knockdown appears to alter the fate determination of spermatocytes, potentially leading to disruptions in spermatogenesis.

Many genes influence meiosis and sperm formation by regulating the ERK pathway. Stra8 is one of the most important genes regulating the initiation of meiosis in spermatocytes. Overexpression of Stra8 lead to a significant

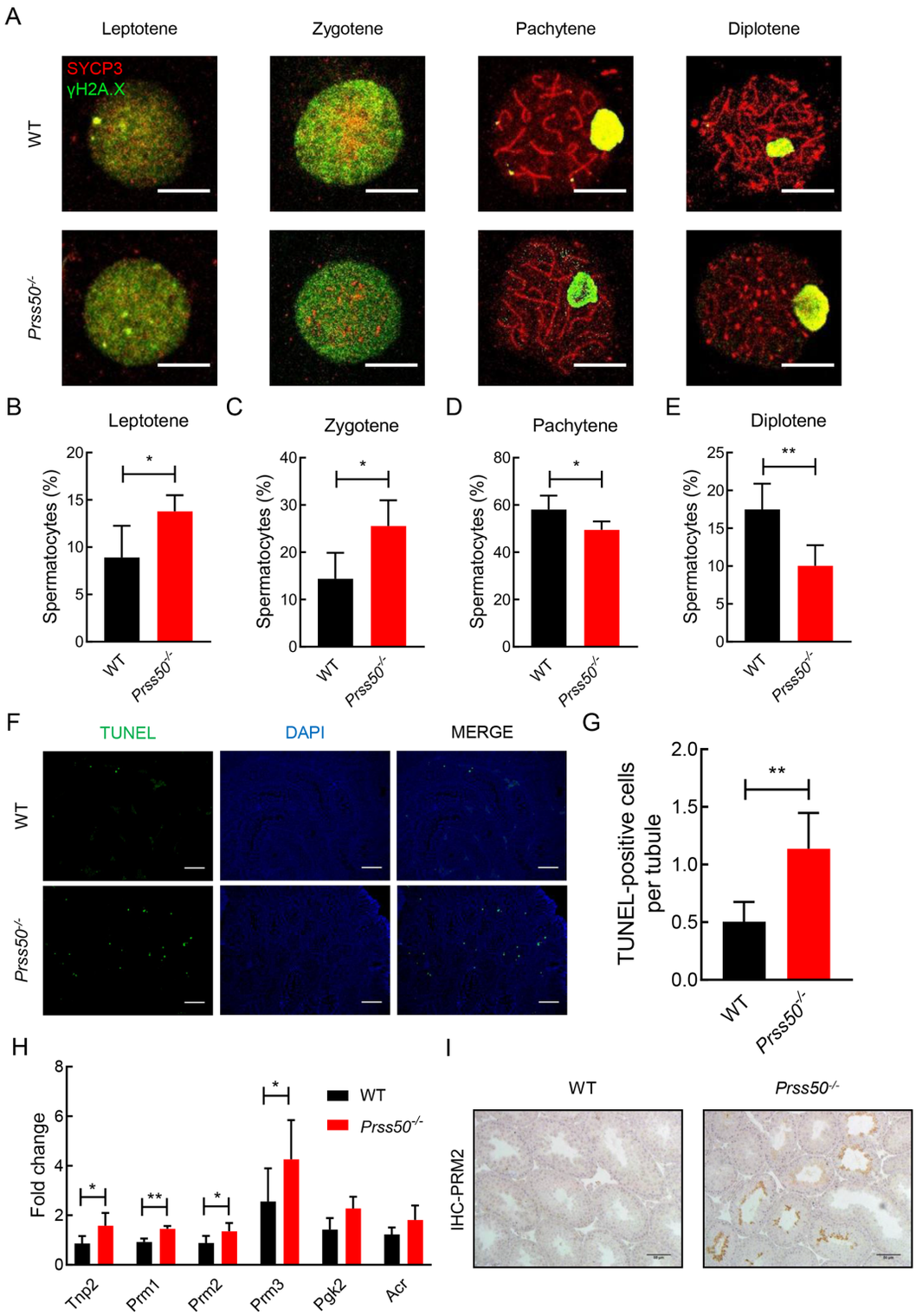

Figure 5 PRSS50 knockout impeded meiotic progression

A–E: *Prss50*$^{-/-}$ mice showed lower proportion of pachytene/diplotene spermatocytes and higher proportion of leptotene/zygotene spermatocytes compared to wild-type mice. Scale bar: 20 μm in A. Quantification of spermatocytes during meiotic prophase stage in wild-type and *Prss50*$^{-/-}$ mice. F, G: TUNEL staining showed increased apoptotic cells in the testis of 4-week-old *Prss50*$^{-/-}$ mice. Scale bar: 50 μm in F. H: qPCR assay showed increased mRNA levels of spermatid markers in the testis of *Prss50*$^{-/-}$ mice. I: Immunohistochemical assay showed premature expression of PRM2 in the testis of 4-week-old *Prss50*$^{-/-}$ mice. Scale bar: 50 μm. Data are mean±SD, ns: Not significant; *: P<0.05; **: P<0.01.

increase in ERK signal activation in GC-1spg cells, suggesting a close relationship between the ERK signaling pathway and the meiotic process (Shen et al., 2018). Additionally, JWH133 can induce ERK1/2 phosphorylation in spermatogonia, promoting their progression toward meiosis (Grimaldi et al., 2009). Activated ERK and p90RSK2 are tightly associated with condensed meiotic chromosomes in spermatocytes (Di Agostino et al., 2004). Additionally, the phosphorylation levels of ERK are positively correlated with AKAP97 function (Jivan et al., 2009). Previous research has reported that deletion of

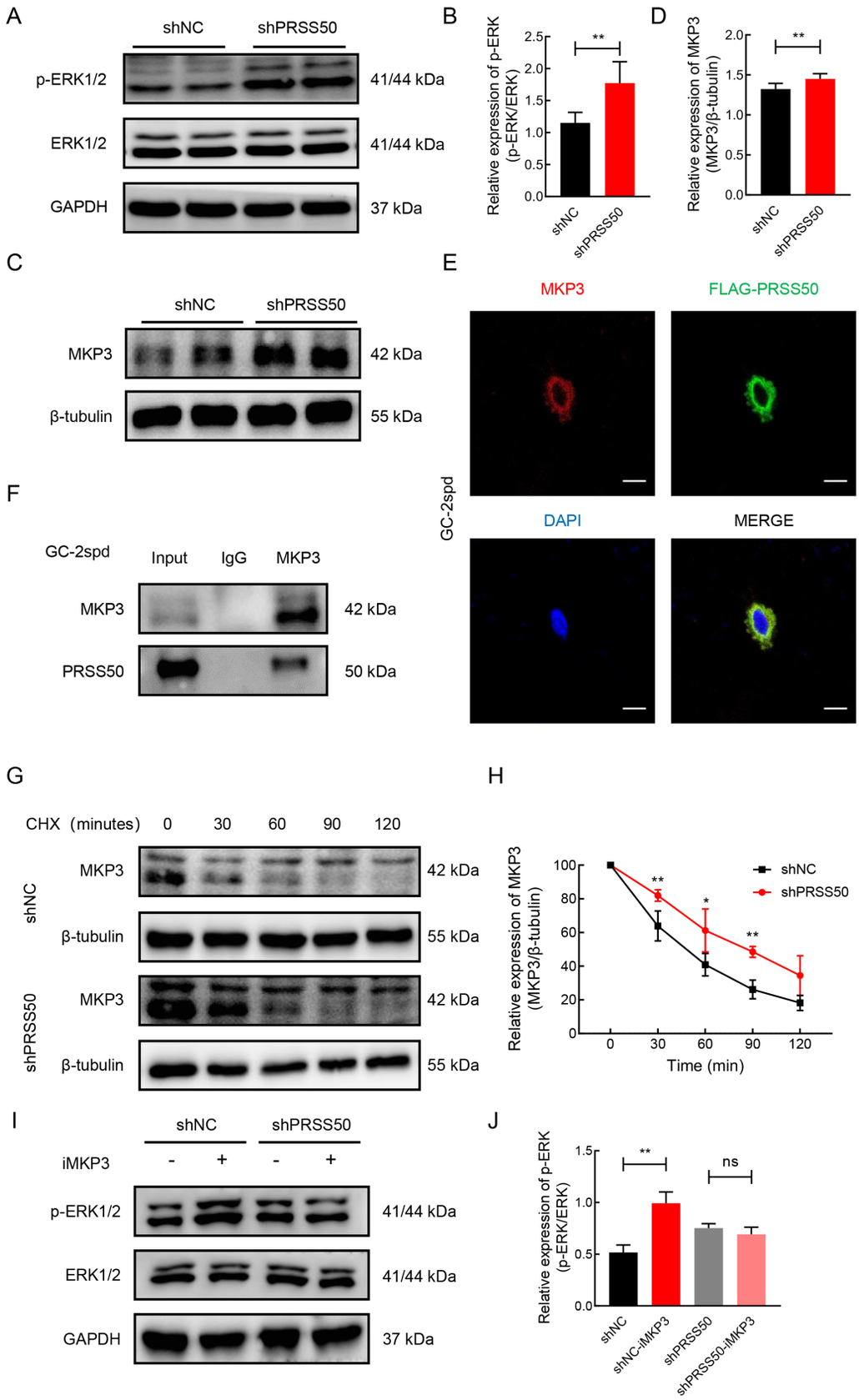

Figure 6 PRSS50 knockdown disturbed MKP3/ERK signaling by binding to MKP3

A, B: Western blot analysis indicated up-regulation of p-ERK1/2 levels in PRSS50-knockdown GC-2spd cells. C, D: Western blot analysis indicated up-regulation of MKP3 levels in PRSS50-knockdown GC-2spd cells. E: PRSS50 co-localized with MKP3 in GC-2spd cells. Scale bar: 20 μm. F: Co-immunoprecipitation assays showed interaction between PRSS50 and MKP3 in GC-2spd cells. G, H: After CHX treatment, MKP3 protein degraded more slowly in PRSS50-knockdown GC-2spd cells compared to control GC-2spd cells. I, J: BCI treatment had no significant effect on levels of p-ERK1/2 protein in PRSS50-knockdown GC-2spd cells. Data are mean±SD, ns: Not significant; *: P<0.05; **: P<0.01.

Prss50 up-regulates AKAP4 protein levels (Scovell et al., 2021). In our study, we observed abnormal activation of ERK in *Prss50*$^{-/-}$ mice, suggesting that AKAP4 levels may be regulated by the ERK signaling pathway.

MKP3 functions as a dephosphorylase of ERK and is involved in the development of various tumors (Gao et al., 2020; Moncho-Amor et al., 2019). MKP3 also affects cell differentiation by regulating ERK activity (Donaubauer et al., 2016; Kim et al., 2015; Zhang et al., 2021). Previous studies have indicated that the negative feedback loop between ERK and MKP3 is regulated by p90RSK2 and CIC (Ren et al., 2020). These observations suggest that MKP3-mediated ERK signaling plays a critical role in meiosis. In our study, *Prss50*$^{-/-}$ mice exhibited increased expression levels of MKP3 and phosphorylated ERK. We propose that the absence of PRSS50 results in the loss of MKP3 phosphatase activity, leading to the accumulation of inactive MKP3 in the cytoplasm and abnormal activation of ERK.

Our findings demonstrated that PRSS50 deficiency in mice resulted in male subfertility, impaired spermatocyte meiosis, and premature expression of haploid cell markers. Mechanistically, PRSS50 interacted with MKP3 and regulated its protein half-life, potentially affecting the diphosphatase activity of MKP3 and activation of the ERK signal pathway.

Overall, this study provides novel insights into PRSS50 and its regulatory mechanisms in testicular development and spermatogenesis. These findings, in conjunction with previous research, contribute to a more comprehensive understanding of the function of PRSS50.

SUPPLEMENTARY DATA

Supplementary data to this article can be found online.

COMPETING INTERESTS

The authors declare that they have no competing interests.

AUTHORS' CONTRIBUTIONS

C.X.N. and J.W.L. contributed equally to this work. C.X.N. and J.W.L. performed the research and wrote the manuscript. X.L.L., L.L.Z., and Y.L. contributed to the knockout mice. C.L.Y. and X.G.Y. conducted data acquisition, analysis, and interpretation. H.F.Z., J.L.S., X.W., and X.H.H. performed data interpretation and statistical analysis. L.H.Z., Y.S., and G.N.W. provided technical and material support. Z.B.S. and Y.L.B. designed the study and revised the paper. All authors read and approved the final version of the manuscript.

ACKNOWLEDGMENTS

We are grateful to Hui-Han Ai from the Tumor Hospital of Zhengzhou University for help in this study.

REFERENCES

Agarwal A, Baskaran S, Parekh N, et al. 2021. Male infertility. *The Lancet*, **397**(10271): 319–333.

Agarwal A, Mulgund A, Hamada A, et al. 2015. A unique view on male infertility around the globe. *Reproductive Biology and Endocrinology*, **13**: 37.

Aoki VW, Liu LH, Jones KP, et al. 2006. Sperm protamine 1/protamine 2 ratios are related to in vitro fertilization pregnancy rates and predictive of fertilization ability. *Fertility and Sterility*, **86**(5): 1408–1415.

Camps M, Nichols A, Arkinstall S. 2000. Dual specificity phosphatases: a gene family for control of MAP kinase function. *The FASEB Journal*, **14**(1): 6–16.

Cao QH, Liu F, Li CZ, et al. 2018. Testes-specific protease 50 (TSP50) promotes invasion and metastasis by inducing EMT in gastric cancer. *BMC Cancer*, **18**(1): 94.

Chen ZG, Kang XJ, Wang LP, et al. 2015. Rictor/mTORC2 pathway in oocytes regulates folliculogenesis, and its inactivation causes premature ovarian failure. *The Journal of Biological Chemistry*, **290**(10): 6387–6396.

Cho C, Jung-Ha H, Willis WD, et al. 2003. Protamine 2 deficiency leads to sperm DNA damage and embryo death in mice. *Biology of Reproduction*, **69**(1): 211–217.

Cho C, Willis WD, Goulding EH, et al. 2001. Haploinsufficiency of protamine-1 or -2 causes infertility in mice. *Nature Genetics*, **28**(1): 82–86.

Clark BJ, Cochrum RK. 2007. The steroidogenic acute regulatory protein as a target of endocrine disruption in male reproduction. *Drug Metabolism Reviews*, **39**(2-3): 353–370.

Di Agostino S, Botti F, Di Carlo A, et al. 2004. Meiotic progression of isolated mouse spermatocytes under simulated microgravity. *Reproduction*, **128**(1): 25–32.

Dolci S, Pellegrini M, Di Agostino S, et al. 2001. Signaling through extracellular signal-regulated kinase is required for spermatogonial proliferative response to stem cell factor. *The Journal of Biological Chemistry*, **276**(43): 40225–40233.

Donaubauer EM, Law NC, Hunzicker-Dunn ME. 2016. Follicle-stimulating hormone (FSH)-dependent regulation of extracellular regulated kinase (ERK) phosphorylation by the mitogen-activated protein (MAP) kinase phosphatase MKP3. *The Journal of Biological Chemistry*, **291**(37): 19701–19712.

Esakky P, Hansen DA, Drury AM, et al. 2015. Cigarette smoke-induced cell cycle arrest in spermatocytes [GC-2spd(ts)] is mediated through crosstalk between *Ahr-Nrf2* pathway and MAPK signaling. *Journal of Molecular Cell Biology*, **7**(1): 73–87.

Falvo S, Santillo A, Baccari GC, et al. 2022. d-aspartate and N-methyl-d-aspartate promote proliferative activity in mouse spermatocyte GC-2 cells. *Reproductive Biology*, **22**(1): 100601.

Gao Y, Li H, Han Q, et al. 2020. Overexpression of DUSP6 enhances chemotherapy-resistance of ovarian epithelial cancer by regulating the ERK signaling pathway. *Journal of Cancer*, **11**(11): 3151–3164.

Gou LT, Kang JY, Dai P, et al. 2017. Ubiquitination-deficient mutations in human *Piwi* cause male infertility by impairing histone-to-protamine exchange during spermiogenesis. *Cell*, **169**(6): 1090–1104. e13.

Grimaldi P, Orlando P, Di Siena S, et al. 2009. The endocannabinoid system and pivotal role of the CB_2 receptor in mouse spermatogenesis. *Proceedings of the National Academy of Sciences of the United States of America*, **106**(27): 11131–11136.

Guida E, Tassinari V, Colopi A, et al. 2022. MAPK activation drives male and female mouse teratocarcinomas from late primordial germ cells. *Journal of Cell Science*, **135**(8): jcs259375.

Hacioglu BM, Kodaz H, Erdogan B, et al. 2017. *K-RAS* and *N-RAS* mutations in testicular germ cell tumors. *Bosnian Journal of Basic Medical Sciences*, **17**(2): 159–163.

Hammoud S, Liu L, Carrell DT. 2009. Protamine ratio and the level of histone retention in sperm selected from a density gradient preparation. *Andrologia*, **41**(2): 88–94.

Hou SY, Xian L, Shi PL, et al. 2016. The *Magea* gene cluster regulates male germ cell apoptosis without affecting the fertility in mice. *Scientific Reports*, **6**: 26735.

Huang B, Butler R, Miao Y, et al. 2016. Dysregulation of Notch and ERα signaling in AhR$^{-/-}$ male mice. *Proceedings of the National Academy of Sciences of the United States of America*, **113**(42): 11883–11888.

Huang Y, Wang YZ, Wang M, et al. 2008. Differential methylation of *TSP50* and *mTSP50* genes in different types of human tissues and mouse spermatic cells. *Biochemical and Biophysical Research Communications*, **374**(4): 658–661.

Jivan A, Earnest S, Juang YC, et al. 2009. Radial spoke protein 3 is a

mammalian protein kinase A-anchoring protein that binds ERK1/2. *The Journal of Biological Chemistry*, **284**(43): 29437–29445.

Kim WK, Oh KJ, Choi HR, et al. 2015. MAP kinase phosphatase 3 inhibits brown adipocyte differentiation via regulation of Erk phosphorylation. *Molecular and Cellular Endocrinology*, **416**: 70–76.

Koskenniemi JJ, Virtanen HE, Toppari J. 2017. Testicular growth and development in puberty. *Current Opinion in Endocrinology, Diabetes, and Obesity*, **24**(3): 215–224.

Lee K, Haugen HS, Clegg CH, et al. 1995. Premature translation of protamine 1 mRNA causes precocious nuclear condensation and arrests spermatid differentiation in mice. *Proceedings of the National Academy of Sciences of the United States of America*, **92**(26): 12451–12455.

Li JW, Niu CX, Ai HH, et al. 2024. TSP50 attenuates DSS-induced colitis by regulating TGF-β signaling mediated maintenance of intestinal mucosal barrier integrity. *Advanced Science*, **11**(11): 2305893.

Liu F, Cao QH, Liu N, et al. 2014. Overexpression of testes-specific protease 50 (TSP50) predicts poor prognosis in patients with gastric cancer. *Gastroenterology Research and Practice*, **2014**: 498246.

Livak KJ, Schmittgen TD. 2001. Analysis of relative gene expression data using real-time quantitative PCR and the 2(-Delta Delta C(T)) Method. *Methods*, **25**(4): 402–408.

Lüke L, Campbell P, Varea Sánchez M, et al. 2014. Sexual selection on protamine and transition nuclear protein expression in mouse species. *Proceedings of the Royal Society B: Biological Sciences*, **281**(1783): 20133359.

Malla AB, Bhandari R. 2017. IP6K1 is essential for chromatoid body formation and temporal regulation of *Tnp2* and *Prm2* expression in mouse spermatids. *Journal of Cell Science*, **130**(17): 2854–2866.

Moghbelinejad S, Najafipour R, Hashjin AS. 2015. Comparison of protamine 1 to protamine 2 mRNA ratio and *YBX2* gene mRNA content in testicular tissue of fertile and azoospermic men. *International Journal of Fertility & Sterility*, **9**(3): 338–345.

Moncho-Amor V, Pintado-Berninches L, Ibañez de Cáceres I, et al. 2019. Role of Dusp6 phosphatase as a tumor suppressor in non-small cell lung cancer. *International Journal of Molecular Sciences*, **20**(8): 2036.

Otsuka K, Matsubara S, Shiraishi A, et al. 2021. A testis-specific long noncoding RNA, *Start*, is a regulator of steroidogenesis in mouse Leydig cells. *Frontiers in Endocrinology*, **12**: 665874.

Perobelli JE. 2014. The male peripubertal phase as a developmental window for reproductive toxicology studies. *Current Pharmaceutical Design*, **20**(34): 5398–5415.

Plant TM, Marshall GR. 2001. The functional significance of FSH in spermatogenesis and the control of its secretion in male primates. *Endocrine Reviews*, **22**(6): 764–786.

Ren YB, Ouyang ZL, Hou ZW, et al. 2020. CIC is a mediator of the ERK1/2-DUSP6 negative feedback loop. *iScience*, **23**(11): 101635.

Scovell JM, Bournat JC, Szafran AT, et al. 2021. PRSS50 is a testis protease responsible for proper sperm tail formation and function. *Development*, **148**(8): dev197558.

Sette C, Barchi M, Bianchini A, et al. 1999. Activation of the mitogen-activated protein kinase ERK1 during meiotic progression of mouse pachytene spermatocytes. *The Journal of Biological Chemistry*, **274**(47): 33571–33579.

Shan JD, Yuan LM, Xiao QX, et al. 2002. TSP50, a possible protease in human testes, is activated in breast cancer epithelial cells. *Cancer Research*, **62**(1): 290–294.

Shang X, Shen CL, Liu JB, et al. 2018. Serine protease PRSS55 is crucial for male mouse fertility via affecting sperm migration and sperm-egg binding. *Cellular and Molecular Life Sciences*, **75**(23): 4371–4384.

Sharma A, Minhas S, Dhillo WS, et al. 2021. Male infertility due to testicular disorders. *The Journal of Clinical Endocrinology & Metabolism*, **106**(2): e442–e459.

Shen CL, Kuang Y, Liu JB, et al. 2013. Prss37 is required for male fertility in the mouse. *Biology of Reproduction*, **88**(5): 123.

Shen CL, Xiong WF, Li CJ, et al. 2022. Testis-specific serine protease PRSS54 regulates acrosomal granule localization and sperm head morphogenesis in mice. *Biology of Reproduction*, **107**(4): 1139–1154.

Shen XY, Niu CM, Guo JQ, et al. 2018. Stra8 may inhibit apoptosis during mouse spermatogenesis via the AKT signaling pathway. *International Journal of Molecular Medicine*, **42**(5): 2819–2830.

Shiraishi K, Matsuyama H. 2017. Gonadotoropin actions on spermatogenesis and hormonal therapies for spermatogenic disorders. *Endocrine Journal*, **64**(2): 123–131.

Sleutels F, Soochit W, Bartkuhn M, et al. 2012. The male germ cell gene regulator CTCFL is functionally different from CTCF and binds CTCF-like consensus sites in a nucleosome composition-dependent manner. *Epigenetics & Chromatin*, **5**(1): 8.

Smith LB, Walker WH. 2014. The regulation of spermatogenesis by androgens. *Seminars in Cell & Developmental Biology*, **30**: 2–13.

Sommerer F, Hengge UR, Markwarth A, et al. 2005. Mutations of *BRAF* and *RAS* are rare events in germ cell tumours. *International Journal of Cancer*, **113**(2): 329–335.

Song ZB, Bao YL, Zhang Y, et al. 2011. Testes-specific protease 50 (TSP50) promotes cell proliferation through the activation of the nuclear factor κB (NF-κB) signalling pathway. *Biochemical Journal*, **436**(2): 457–467.

Takebe M, Onohara Y, Yokota S. 2013. Expression of MAEL in nuage and non-nuage compartments of rat spermatogenic cells and colocalization with DDX4, DDX25 and MIWI. *Histochemistry and Cell Biology*, **140**(2): 169–181.

Tassinari V, Campolo F, Cesarini V, et al. 2015. Fgf9 inhibition of meiotic differentiation in spermatogonia is mediated by Erk-dependent activation of Nodal-Smad2/3 signaling and is antagonized by Kit Ligand. *Cell Death & Disease*, **6**(3): e1688.

Traven E, Ogrinc A, Kunej T. 2017. Initiative for standardization of reporting genetics of male infertility. *Systems Biology in Reproductive Medicine*, **63**(1): 58–66.

Vasileva A, Tiedau D, Firooznia A, et al. 2009. Tdrd6 is required for spermiogenesis, chromatoid body architecture, and regulation of miRNA expression. *Current Biology*, **19**(8): 630–639.

Xu HP, Yuan LM, Shan JD, et al. 2004. Localization and expression of *TSP50* protein in human and rodent testes. *Urology*, **64**(4): 826–832.

Yoneda R, Takahashi T, Matsui H, et al. 2013. Three testis-specific paralogous serine proteases play different roles in murine spermatogenesis and are involved in germ cell survival during meiosis. *Biology of Reproduction*, **88**(5): 118.

Yuan J, Wu CF, Huang ML, et al. 2015. TSP50 depends on its threonine protease activity and its interactions with TNF-α-induced NF-κB for its role in human cervical tumorigenesis. *Cell Biochemistry and Biophysics*, **71**(2): 891–896.

Zhang BY, Yuan PT, Xu G, et al. 2021. DUSP6 expression is associated with osteoporosis through the regulation of osteoclast differentiation via ERK2/Smad2 signaling. *Cell Death & Disease*, **12**(9): 825.

Zheng L, Xie GF, Duan GJ, et al. 2011. High expression of testes-specific protease 50 is associated with poor prognosis in colorectal carcinoma. *PLoS One*, **6**(7): e22203.

Zhu F, Li W, Zhou XL, et al. 2021. PRSS55 plays an important role in the structural differentiation and energy metabolism of sperm and is required for male fertility in mice. *Journal of Cellular and Molecular Medicine*, **25**(4): 2040–2051.